

Durham Research Online

Deposited in DRO:

07 December 2010

Version of attached file:

Published Version

Peer-review status of attached file:

Peer-reviewed

Citation for published item:

Pugh, S.K. and Dugdale, D.J. and Brand, S. and Abram, R.A. (1999) 'Band-gap and k.p. parameters for GaAlN and GaInN alloys.', *Journal of applied physics.*, 86 (7). pp. 3768-3772.

Further information on publisher's website:

<http://dx.doi.org/10.1063/1.371285>

Publisher's copyright statement:

Copyright (1999) American Institute of Physics. This article may be downloaded for personal use only. Any other use requires prior permission of the author and the American Institute of Physics. The following article appeared in Pugh, S.K. and Dugdale, D.J. and Brand, S. and Abram, R.A. (1999) 'Band-gap and k.p. parameters for GaAlN and GaInN alloys.', *Journal of applied physics.*, 86 (7). pp. 3768-3772 and may be found at <http://dx.doi.org/10.1063/1.371285>

Additional information:

Use policy

The full-text may be used and/or reproduced, and given to third parties in any format or medium, without prior permission or charge, for personal research or study, educational, or not-for-profit purposes provided that:

- a full bibliographic reference is made to the original source
- a [link](#) is made to the metadata record in DRO
- the full-text is not changed in any way

The full-text must not be sold in any format or medium without the formal permission of the copyright holders.

Please consult the [full DRO policy](#) for further details.

Band-gap and $\mathbf{k}\cdot\mathbf{p}$ parameters for GaAlN and GaInN alloys

S. K. Pugh, D. J. Dugdale,^{a)} S. Brand, and R. A. Abram

Department of Physics, University of Durham, South Road, Durham, DH1 3LE, United Kingdom

(Received 25 January 1999; accepted for publication 20 April 1999)

Using a semi-empirical pseudopotential method, a set of band-structure calculations are performed on a range of GaInN and GaAlN alloys in both the zinc-blende and wurtzite structures. Pseudopotentials for the bulk materials are described by suitable $V(q)$ functions, and these are used to construct the alloy pseudopotentials. The band gap as a function of alloy composition is studied, and it is found that there is no significant bowing in the case of GaAlN. The bowing is larger for GaInN, although heavily dependent on the strain present. A more detailed study of the wurtzite alloys is carried out for low Al and In fractions. Wurtzite $\mathbf{k}\cdot\mathbf{p}$ parameters for several alloys at concentrations commonly used in devices are obtained from the semi-empirical band structure using a Monte Carlo fitting procedure. © 1999 American Institute of Physics. [S0021-8979(99)02415-9]

I. INTRODUCTION

There is currently a great deal of interest in group-III nitride compounds and alloys due to their potential technological importance, particularly for blue-green light emitting devices.¹ As an aid in the optimization of the electronic and/or optical properties of optical sources, accurate band-structure information is required for the various layers of material, under the appropriate strains, which make up the device. Unfortunately, there is limited experimental information available on the electronic structure of the alloys relevant to the devices that are currently the center of attention. It would, therefore, be particularly helpful to obtain theoretical band structure, as well as parameters for band-structure models which can form the basis for calculations of the optical properties and for device modeling and design.

Despite the problems with the growth of group-III nitrides, there has been much improvement in the quality of samples of the compounds. As a result, increasingly accurate measurements of some physical quantities have been made including lattice parameters,²⁻⁴ principal band gaps,⁵⁻⁷ and splitting energies of bands.⁸⁻¹⁰ The experimental activity has continued to stimulate theoretical studies of the electronic structure of these materials.¹¹ There have been a large number of theoretical studies of the compounds, including first-principles,¹² semi-empirical pseudopotential,¹³ and $\mathbf{k}\cdot\mathbf{p}$ ^{14,15} calculations. However, there has been much less work on the GaAlN and GaInN alloys, and little information on their band-structure exists.

In this theoretical work, a semi-empirical pseudopotential method is used to obtain potentials for the compounds that form the basis of band-structure calculations for the alloys. In this article we report the results of calculations of the principal band gap of GaAlN and GaInN alloys over the full range of possible compositions and for both wurtzite and zinc-blende structures. In addition, $\mathbf{k}\cdot\mathbf{p}$ parameters have been obtained for a number of wurtzite alloys that are relevant to devices.

II. RESULTS

In earlier work, the authors performed band-structure calculations on bulk nitride materials¹¹ using the semi-empirical pseudopotential method. Here, we use a similar approach to study the electronic structure of GaInN and GaAlN alloys in both the zinc-blende and wurtzite forms. The theoretical framework used is essentially the pseudopotential method of Cohen and Chelikowsky.¹⁶ Supporting first-principles calculations have also been performed using VASP, a density functional theory-pseudopotential based code.¹⁷⁻¹⁹

The semi-empirical pseudopotential form factors, $V(\mathbf{G})$, are derived from a suitable constructed $V(q)$ function. This function is obtained for GaN, AlN, and InN using a Monte Carlo approach which adjusts the parameters of the function until the band structure is in good agreement with experimental and first-principles results for unstrained material. The advantage of using such a function is that it provides a versatile platform for deriving pseudopotentials representing strained materials and alloys. The equations describing the symmetric V_s and antisymmetric V_a parts of the pseudopotential (in Rydbergs) are defined in Eq. (1), in which q is in units of $(2\pi/a_{zb})$ where a_{zb} is the equilibrium lattice parameter in zinc-blende.

$$V_s = \frac{a_1 q^2 + a_2}{1 + \exp(a_3[a_4 - q^2])}, \quad (1)$$

$$V_a = (a_{1q} + a_2) \exp(a_3[a_4 - q^2]).$$

For each of the three compounds GaN, AlN, and InN, in both crystal structures, semiempirical pseudopotentials have been generated by fitting energy eigenvalues to band-structure data from experiment and first-principles calculations (notably Rubio *et al.*¹²) through variation of the a_i , $i = 1...4$. This is the same procedure described in our previous work,¹¹ and the pseudopotentials used here for zinc-blende are identical. New sets of values of a_i have been obtained for the wurtzite structures. The coefficients of the $V(q)$ functions obtained are shown in Table I.

^{a)}Electronic mail: D.J.Dugdale@durham.ac.uk

TABLE I. The coefficients of the form-factor $V(q)$ functions. The functions are defined in Eq. (1)

	V_s				V_a			
	a_1	a_2	a_3	a_4	a_1	a_2	a_3	a_4
ZB								
GaN	0.0752	-0.517	-0.526	10.074	0.0101	0.082	0.107	8.836
AlN	0.0769	-0.424	-0.370	10.496	0.0209	0.094	0.116	10.427
InN	0.0732	-0.527	-0.573	9.507	0.0052	0.079	0.102	8.267
WZ								
GaN	0.0837	-0.564	-0.549	10.508	0.0015	0.087	0.127	10.508
AlN	0.0767	-0.448	-0.483	10.755	0.0018	0.101	0.174	10.737
InN	0.0843	-0.610	-0.585	10.375	0.0079	0.086	0.049	9.644

Since the effect of strain is important in the current work, a series of calculations have been performed in order to calculate band-gap deformation potentials, a_g . These are defined as

$$a_g = \frac{dE_g}{d\log\Omega}, \quad (2)$$

where E_g is the band gap, and Ω is the unit-cell volume. Using the continuous $V(q)$ description for the pseudopotential, a set of form factors can be obtained which represent the hydrostatically strained bulk material. This is achieved by determining the values of the scaled $V(q)$ function for the strained unit cell volume, at the associated strained G values. For comparison, the deformation potentials were also calculated from first principles, using VASP. The results obtained using the two theoretical approaches, together with those from the literature, are shown in Table II. They show that for the zinc-blende materials, our semi-empirical approach tends to produce larger values than the first-principles calculations. For the wurtzite materials, there is close agreement for AlN but the semi-empirical result for GaN is rather smaller. However, there is little reliable information available from experiment, and the theoretical results are not always consistent.

TABLE II. The band-gap deformation potential (eV) obtained using both first-principles and semi-empirical approaches. Other results taken from theory (see footnotes b-d) or an experiment/theory combination (see footnotes a and e for explanation) are also shown.

Material	First-prin.	Semi-emp.	Others
ZB GaN	-7.0	-11.2	-8.8 ^b , -7.4 ^a
AlN	-9.0	-14.6	-7.7 ^b , -6.4 ^c
InN	...	-7.7	-3.0 ^c
WZ GaN	-6.8	-11	-7.8 ^c , -9.8 ^c , -6.9 ^b
AlN	-9.0	-12.4	-7.1 to -9.5 ^c
InN	...	-9.1	-4.2 ^c

^aSee Ref. 20.

^bSee Ref. 13.

^cSee Ref. 21.

In order to calculate the band structure of our virtual crystal ternary alloy, appropriate form factors are derived from the $V(q)$ functions for the relevant binary compounds. The alloy lattice constant, and hence, the appropriate unit-cell volume and G values for the alloy, are obtained using Vegard's Law, and represent unstrained material. Both the symmetric and antisymmetric form factors for the $A_{1-x}B_xN$ alloy at a given G are given by the expression

$$V_{\text{alloy}}(G) = V_A(G)(1-x) + V_B(G)x, \quad (3)$$

where the individual $V_A(G)$, $V_B(G)$ are obtained using Eq. (1) at the alloy G values. In effect, due to the different lattice constants of the original A, B compounds and the binary alloys, this amounts to a shift along the $V(q)$ curves from the original $V_{A,B}$, followed by a weighted averaging.

For the case of $\text{Ga}_{0.5}\text{In}_{0.5}\text{N}$, Fig. 1 shows the antisymmetric form factors obtained as pluses and the symmetric form factors as crosses. Also shown are the compound form factors (indicated by circles and squares for InN and GaN, respectively), and the $V(q)$ curves from which the alloy form factors are derived.

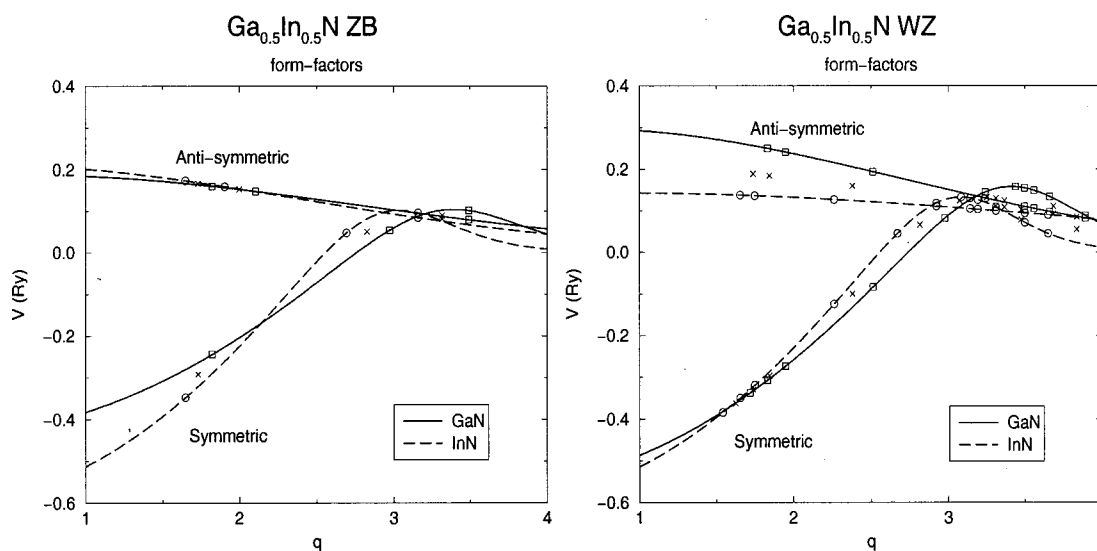


FIG. 1. The symmetric and antisymmetric form factors for the $\text{Ga}_{0.5}\text{In}_{0.5}\text{N}$ alloy calculated from the $V(q)$ curves of bulk GaN and InN. The left panel is for zinc-blende and the right panel for wurtzite. The alloy form factors are indicated by crosses (antisymmetric) and pluses (symmetric).

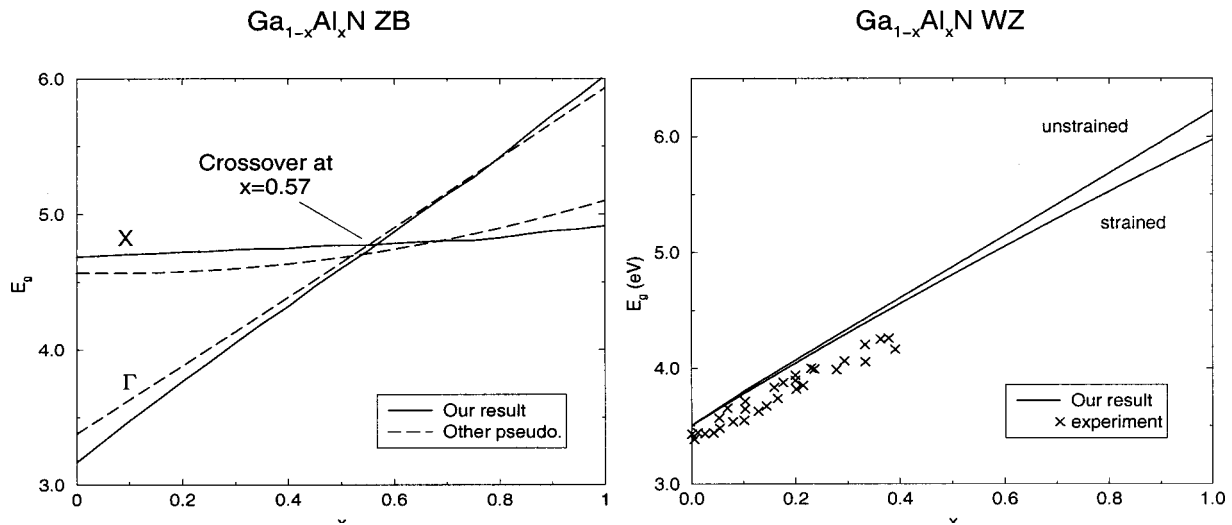


FIG. 2. The band gap E_g as a function of alloy composition x in $\text{Ga}_{1-x}\text{Al}_x\text{N}$. For the zinc-blende material (left panel), the band gap at both the Γ and X points are shown, together with the results of another semi-empirical pseudopotential calculation (see Ref. 13). The wurtzite material (right panel) is shown with a comparison to experimental data compiled in Ref. 23.

In addition, for the wurtzite structure, biaxially strained material has been considered. For GaAlN and GaInN, the in-plane lattice parameter a has been held at the GaN value (3.19 Å), corresponding to the situation of the alloy being grown on a GaN substrate. The corresponding perpendicular lattice parameter c was calculated using the first-principles code. The values of c obtained with $a=3.19$ Å were: for InN, $c=6.288$ Å; and for AlN, $c=4.736$ Å. The c parameter for a given alloy was then obtained by a linear interpolation.

Form factors for the full range of $\text{Ga}_{1-x}\text{Al}_x\text{N}$ and $\text{Ga}_{1-x}\text{In}_x\text{N}$ alloys have been calculated, and are used in the band-structure calculations. For the zinc-blende materials, the unstrained alloys only have been considered, but for wurtzite, both strained and unstrained calculations have been performed. Of particular interest are the band gaps as a func-

tion of alloy composition x , and these are shown in Fig. 2 for the GaAlN alloy, and Fig. 3 for the GaInN alloy.

Our calculations predict that the band gap varies almost linearly with composition in zinc-blende $\text{Ga}_{1-x}\text{Al}_x\text{N}$. As the conduction band energy at the X point is also plotted on this diagram, the direct-indirect crossover can be seen. It is found that this occurs at an Al fraction $x=0.57$, in agreement with other calculations.^{13,22} In the wurtzite case, the inclusion of strain has little effect on GaAlN but somewhat more for GaInN, where there is significant bowing as in the zinc-blende case. Also shown on this figure are some experimental data (labelled A) compiled from various sources,²³ and further experimental data (labelled B) valid for strained $\text{Ga}_{1-x}\text{In}_x\text{N}$ grown on GaN, with $x \leq 0.12$.²⁴ Note that there is a slight offset in the value of E_g at $x=0$ due to our original

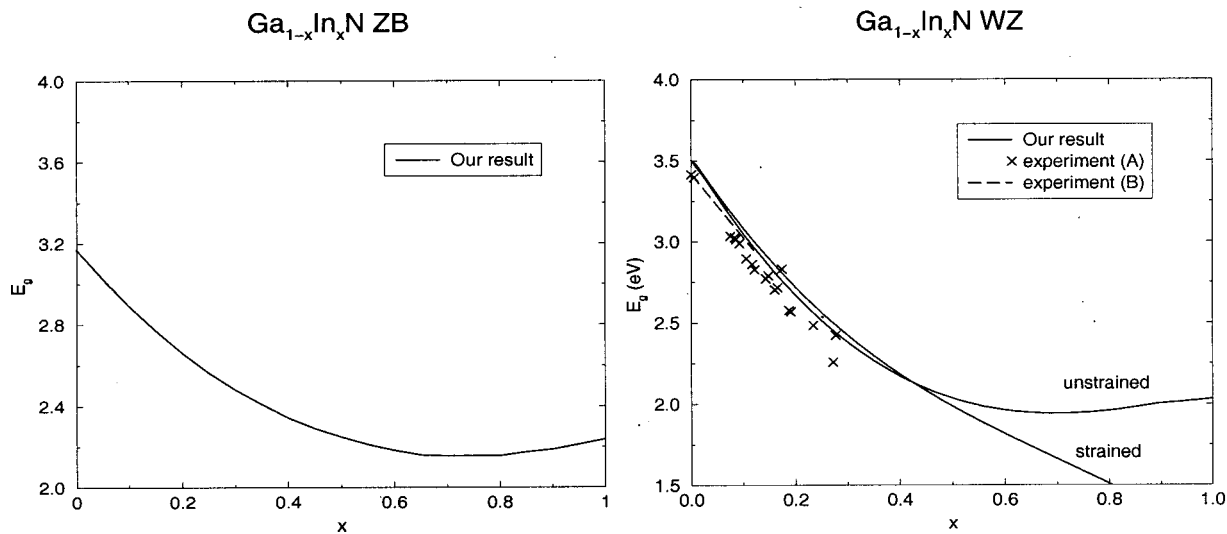


FIG. 3. The band gap E_g as a function of alloy composition x in $\text{Ga}_{1-x}\text{In}_x\text{N}$. The zinc-blende material is shown in the left panel and the wurtzite on the right. In the wurtzite case, also shown are experimental data points (A) compiled in Ref. 23 and corrected experimental data (B) representing an unstrained alloy (see Ref. 24).

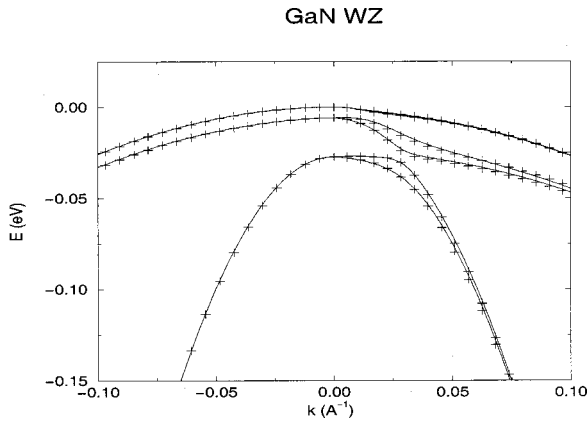


FIG. 4. Band structure for wurtzite GaN near the Γ point. The crosses indicate the results from the semi-empirical results, and the solid line are those from the $\mathbf{k}\cdot\mathbf{p}$ method.

GaN fit, but that the actual gradients are in good agreement for both alloys. Recent additional experimental results for small x ^{25,26} show similar trends. Other theoretical work²⁷ attributes the large band-gap bowing to In-localized hole states in the upper valence band rather than the large lattice mismatch between the two materials. Our model cannot represent this, but nevertheless appears to give a good description of the band-gap bowing.

The $\mathbf{k}\cdot\mathbf{p}$ band-structure method¹⁵ is particularly useful for modeling the electronic structure and optical properties of simple heterostructures and devices. A set of $\mathbf{k}\cdot\mathbf{p}$ parameters have been derived for each of the three wurtzite compounds using our pseudopotential results. These consist of A_i ($i=1\dots7$) parameters which determine the shape of the bands, and Δ_i ($i=1\dots3$) parameters which determine splitting energies. The parameter A_7 is often neglected but Ren, Liu, and Blood²⁷ have recently shown how the lifting of the degeneracy of the valence bands near the anticrossing feature can be modeled extremely well by its inclusion, and hence, is also used here.

The technique involved using a Monte Carlo approach to fit the $\mathbf{k}\cdot\mathbf{p}$ parameters to the semi-empirical band structure for each material. The $\mathbf{k}\cdot\mathbf{p}$ parameters used for the wurtzite materials are shown in Table III, and a plot of the band structure for GaN near the Γ point is shown in Fig. 4.

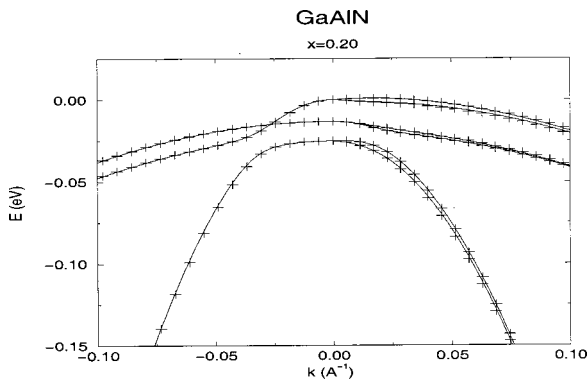


FIG. 5. Band structure for $\text{Ga}_{0.80}\text{Al}_{0.20}\text{N}$ near the Γ point. The crosses indicate the results from the semi-empirical results, and the solid lines are those from the $\mathbf{k}\cdot\mathbf{p}$ method.

TABLE III. Wurtzite $\mathbf{k}\cdot\mathbf{p}$ parameters for bulk GaN, AlN, and InN. The A_i are in units of $\hbar^2/2m_0$ except A_7 where the units are $\text{eV}\text{\AA}^{-1}$.

	GaN	AlN	InN
E_g (eV)	3.50	6.22	2.03
A_1	-7.71	-4.61	-9.65
A_2	-0.60	-0.54	-0.71
A_3	7.02	4.10	8.96
A_4	-3.08	-1.59	-4.17
A_5	-3.04	-1.76	-4.18
A_6	-4.00	-2.15	-5.37
A_7	-0.19	-0.19	-0.33
$m_c^p(m_0)$	0.15	0.25	0.10
$m_c^v(m_0)$	0.14	0.24	0.10
Δ_1 (meV)	22.3	-93.2	37.3
Δ_2 (meV)	3.7	3.7	3.7

For several specific wurtzite alloy concentrations, the band structure was studied in more detail and a set of $\mathbf{k}\cdot\mathbf{p}$ parameters derived, using a method identical to that for the compounds. The alloys chosen were of small Al or In fraction, as these are the most commonly used in quantum well devices. For $\text{Ga}_{1-x}\text{In}_x\text{N}$, the In fractions considered were $x=0.05, 0.08, 0.10,$ and 0.15 . For $\text{Ga}_{1-x}\text{Al}_x\text{N}$, the Al fractions chosen were $x=0.05, 0.08, 0.10, 0.15,$ and 0.20 . The $\mathbf{k}\cdot\mathbf{p}$ parameters are shown in Table IV for GaAlN and Table V for GaInN. In addition, band-structure plots for $\text{Ga}_{0.80}\text{Al}_{0.20}\text{N}$ and $\text{Ga}_{0.85}\text{In}_{0.15}\text{N}$ are shown in Figs. 5 and 6. The original pseudopotential band structure and fitted $\mathbf{k}\cdot\mathbf{p}$ results are in good agreement in most cases, and particularly so at small wave vector. Note that there is a flip over in the normal ordering of the bands for $\text{Ga}_{0.85}\text{In}_{0.15}\text{N}$.

III. CONCLUSION

A series of semi-empirical pseudopotentials have been derived which correspond to a range of GaAlN and GaInN alloys of wurtzite and zinc-blende structure. These have been used to study the band-gap as a function of alloy composi-

TABLE IV. Wurtzite $\mathbf{k}\cdot\mathbf{p}$ parameters for $\text{Ga}_{1-x}\text{Al}_x\text{N}$, with Al fraction x ranging from 0.05 to 0.20. The A_i are in units of $\hbar^2/2m_0$ except A_7 where the units are $\text{eV}\text{\AA}^{-1}$.

	$\text{Ga}_{1-x}\text{Al}_x\text{N}$				
	$x=0.05$	$x=0.08$	$x=0.10$	$x=0.15$	$x=0.20$
E_g (eV)	3.65	3.74	3.79	3.93	4.07
A_1	-7.26	-7.17	-7.08	-6.87	-6.67
A_2	-0.60	-0.62	-0.65	-0.57	-0.57
A_3	6.56	6.50	6.41	6.21	6.02
A_4	-2.97	-2.87	-2.77	-2.79	-2.67
A_5	-2.97	-2.91	-2.89	-2.75	-2.66
A_6	-3.88	-3.88	-3.82	-3.68	-3.50
A_7	-0.19	-0.18	-0.17	-0.17	-0.17
$m_c^p(m_0)$	0.15	0.15	0.16	0.16	0.17
$m_c^v(m_0)$	0.14	0.15	0.15	0.15	0.16
Δ_1 (meV)	13.6	6.2	2.4	-7.0	-16.1
Δ_2 (meV)	3.6	4.4	4.5	4.7	4.9

TABLE V. Wurtzite $\mathbf{k}\cdot\mathbf{p}$ parameters for $\text{Ga}_{1-x}\text{In}_x\text{N}$, with In fraction x ranging from 0.05 to 0.15. The A_i are in units of $\hbar^2/2m_0$ except A_7 where the units are $\text{eV}\text{\AA}^{-1}$.

	$\text{Ga}_{1-x}\text{In}_x\text{N}$			
	$x=0.05$	$x=0.08$	$x=0.10$	$x=0.15$
E_g (eV)	3.28	3.14	3.05	2.85
A_1	-7.91	-8.12	-8.27	-8.64
A_2	-0.65	-0.68	-0.70	-0.77
A_3	7.22	7.43	7.57	7.93
A_4	-3.15	-3.17	-3.20	-3.25
A_5	-3.16	-3.22	-3.27	-3.37
A_6	-4.09	-4.19	-4.25	-4.42
A_7	-0.27	-0.31	-0.33	-0.40
$m_v^p(m_0)$	0.14	0.13	0.13	0.13
$m_v^z(m_0)$	0.13	0.13	0.13	0.12
Δ_1 (meV)	-20.2	-42.3	-55.7	-84.6
Δ_2 (meV)	3.8	3.8	3.8	3.8

tion, and it is found that while there is little or no band-gap bowing in GaAlN, there is significant bowing for GaInN. The direct-to-indirect crossover in zinc-blende GaAlN is predicted to occur at an Al fraction of 0.57. The band-structure results have been used to obtain $\mathbf{k}\cdot\mathbf{p}$ parameters for a number of GaInN and GaAlN alloy compositions of the wurtzite

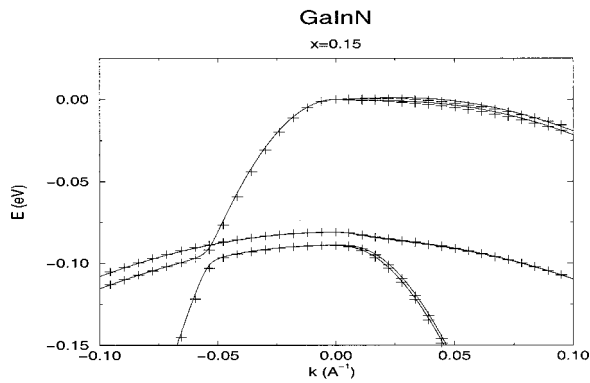


FIG. 6. Band structure for $\text{Ga}_{0.85}\text{In}_{0.15}\text{N}$ near the Γ point. The crosses indicate the results from the semi-empirical results, and the solid lines are those from the $\mathbf{k}\cdot\mathbf{p}$ method.

structure, and will constitute a useful starting point for modeling quantum well devices.

ACKNOWLEDGMENTS

The authors would like to thank EPSRC for supporting SKP on Grant No. GR/L05570 and for the provision of a studentship for DJD. We also thank Dr. G. Kresse and Professor J. Hafner for the provision of the VASP code. We are grateful to Dr. G. B. Ren and Professor P. Blood for communicating the $\mathbf{k}\cdot\mathbf{p}$ results of Ref. 27 prior to publication.

- ¹*The Blue Laser Diode*, edited by S. Nakamura and G. Fasol (Springer, Berlin, 1997).
- ²H. Schulz and K. H. Thiemann, *Solid State Commun.* **23**, 815 (1977).
- ³A. F. Wright and J. S. Nelson, *Phys. Rev. B* **51**, 7866 (1995).
- ⁴I. Gorczyca and N. E. Christensen, *Physica B* **185**, 410 (1993).
- ⁵T. Lei, M. Fanciulli, R. J. Molnar, T. D. Moustakas, R. J. Graham, and J. Scanlon, *Appl. Phys. Lett.* **95**, 944 (1991).
- ⁶*Numerical Data and Functional Relationships in Science and Technology*, Landolt-Börnstein Tables Vol. III/17a, edited by K. H. Hellwege (Springer, New York, 1982).
- ⁷R. Dingle, D. D. Sell, S. E. Stokowski, and M. Ilegems, *Phys. Rev.* **4**, 1211 (1971).
- ⁸J. W. Orton, *Semicond. Sci. Technol.* **11**, 1026 (1996).
- ⁹G. D. Chen, M. Smith, J. Y. Lin, H. X. Jiang, S. H. Wei, M. Asif Khan, and C. J. Sun, *Appl. Phys. Lett.* **68**, 2784 (1996).
- ¹⁰N. V. Edwards *et al.*, *Appl. Phys. Lett.* **70**, 2001 (1997).
- ¹¹S. K. Pugh, D. J. Dugdale, S. Brand, and R. A. Abram, *Semicond. Sci. Technol.* **14**, 23 (1999).
- ¹²A. Rubio, J. L. Corkhill, M. L. Cohen, E. L. Shirley, and S. G. Louie, *Phys. Rev. B* **48**, 11810 (1993).
- ¹³W. J. Fan, M. H. Li, T. C. Chong, and J. B. Xia, *J. Appl. Phys.* **79**, 188 (1996).
- ¹⁴M. Suzuki, T. Uenoyama, and A. Yanase, *Phys. Rev. B* **52**, 8132 (1995).
- ¹⁵S. L. Chuang and C. S. Chang, *Phys. Rev. B* **54**, 2491 (1996).
- ¹⁶J. R. Chelikowsky and M. L. Cohen, *Phys. Rev. B* **14**, 556 (1976).
- ¹⁷G. Kresse and J. Hafner, *Phys. Rev. B* **47**, 558 (1993).
- ¹⁸G. Kresse and J. Furthmüller, *Comput. Mater. Sci.* **6**, 15 (1996).
- ¹⁹G. Kresse and J. Furthmüller, *Phys. Rev. B* **54**, 11169 (1996).
- ²⁰N. E. Christensen and I. Gorczyca, *Phys. Rev. B* **50**, 4397 (1994).
- ²¹K. Kim, W. R. L. Lambrecht, and B. Segall, *Phys. Rev. B* **53**, 16310 (1996).
- ²²E. A. Albanesi, W. R. L. Lambrecht, and B. Segall, *Phys. Rev. B* **48**, 17841 (1993).
- ²³M. J. Bergmann and H. C. Casey, *J. Appl. Phys.* **84**, 1196 (1998).
- ²⁴M. D. McCluskey, C. G. Van de Walle, C. P. Master, L. T. Romano, and N. M. Johnson, *Appl. Phys. Lett.* **72**, 2725 (1998).
- ²⁵C. Wetzel, T. Takeuchi, S. Yamaguchi, H. Katoh, H. Amano, and I. Akasaki, *Appl. Phys. Lett.* **73**, 1994 (1998).
- ²⁶W. Shan *et al.*, *J. Appl. Phys.* **84**, 4452 (1998).
- ²⁷G. B. Ren, Y. M. Liu, and P. Blood, *Appl. Phys. Lett.* (submitted).